JOURNAL OF GUIDANCE, CONTROL, AND DYNAMICS
Vol. 32, No. 4, July–August 2009

Feedback Dual Controller Design and Its Application to Monocular Vision-Based Docking

Jinwhan Kim*
Optimal Synthesis, Inc., Los Altos, California 94022
and
Stephen Rock†
Aerospace Robotics Laboratory, Stanford University, Stanford, California 94305

DOI: 10.2514/1.41957

A novel stochastic feedback control approach, which is capable of considering the presence of uncertainty during the controller design phase, is developed and applied to the automatic docking problem for an unmanned vehicle with a monocular vision sensor. A typical procedure for linear stochastic control employs a two-step approach that separates estimation and control: estimate the system state using noise corrupted measurements, and control the system based on the estimated state. However, for nonlinear stochastic control systems and adaptive control systems with uncertain parameters, control and estimation are often not separable because control inputs can affect not only the system state but also the quality of the state estimation. Dynamic programming and search-based methods are general solution techniques for solving these types of control problems, however, those solution techniques are often infeasible for real-time applications due to the huge computational requirements even for small problems. In this paper, a new systematic, suboptimal control algorithm is presented, which can be implemented as an online feedback controller for a stochastic control problem of moderate dimension. For an application example, automated docking of a nonholonomic vehicle with a monocular vision sensor is considered. The results from a series of numerical simulations and experimental tests are presented.

I. Introduction

MOST dynamic systems operate under the influence of uncertainties, such as environmental disturbance and measurement noise, and, because of this, their control laws must be based on best estimates of their system states. Typical control strategies are based on the certainty equivalence (CE) assumptions that the choice of control actions does not affect nor is it affected by the estimation uncertainty. This leads to a two-step approach: estimate the state of the dynamic system from noise corrupted measurements using a state estimator such as the Kalman filter, and calculate control inputs assuming that those estimated states are true, using a conventional control technique that is valid for deterministic systems. This approach often works quite well and is, in fact, optimal in the sense of minimum mean square error if the system is observable and the linear quadratic Gaussian (LQG) assumptions apply. That is, the system is linear, the cost criterion is quadratic, and the noise is Gaussian. However, the assumptions may not hold for a control system that involves nonlinearities or for an adaptive control system that contains uncertain system parameters in its dynamics.

To achieve better performance for these types of control systems, so-called dual effects need to be considered. This concept was discussed by Feldbaum [1,2]. He pointed out that the control input has two purposes that may conflict with each other. One is to achieve the control goal of system stabilization, and the other is to improve knowledge of any unknown parameters and/or the state of the system [3]. When these conflicting control goals are closely coupled and not separable, the quality of estimation affects the quality of control and vice versa. Dynamic programming and search-based approaches are the general solution techniques for solving this type of control problem. However, in many cases, those solution techniques are practically of little use, because the computational burden even for a small problem is commonly prohibitive [4,5].

In this study, a new stochastic control algorithm is suggested that incorporates a cost incurred by the system uncertainty into the performance index and applies a linear quadratic control technique, which provides a linear feedback control law with the quadratic performance index considering the dual features. This will be abbreviated hence as LQD. The algorithm can be implemented as a real-time controller even for a stochastic control problem of moderate dimension through a systematic design procedure.

This newly designed controller is applied to monocular vision-based docking of an unmanned vehicle. A monocular vision sensor contains a great amount of information, but has a fundamental limitation as a stand-alone position-sensing device due to its nature of bearings-only sensing. Estimation performance in the range direction is heavily affected by vehicle trajectories, and the problem falls into the category of the dual-control problem. That is, the problem has two competing control objectives: the vehicle needs to keep its line-of-sight (LOS) angle close to zero and, at the same time, must swerve from the LOS direction to improve observability of the target location. Conventional CE controllers perform poorly for this type of problem, especially when the vehicle is initially aligned to the LOS line to the target. A series of simulations and experimental results demonstrates the validity of the developed control technique and its real-time capability.

Section II provides a basic problem statement of the generalized optimal stochastic control problem, and Sec. III summarizes existing approaches to solve these types of problems. Section IV describes the details of the proposed LQD techniques and the associated controller design procedure. In Sec. V, the LQD algorithm is applied to monocular vision-based docking, and its simulation and experimental results are shown in Secs. VI and VII, respectively. Conclusions are presented in Sec. VIII.

II. Problem Statement: Optimal Stochastic Control

The general problem considered in this paper is a nonlinear stochastic system described by following equations of states and

Presented as Paper 6090 at the AIAA Guidance, Navigation, and Control Conference, Keystone, CO, 21–24 August 2006; received 1 November 2008; revision received 18 February 2009; accepted for publication 18 February 2009.

*Research Scientist, 95 First Street, Suite 240. Senior Member AIAA.
†Professor, Department of Aeronautics and Astronautics, Durand Building, 496 Lomita Mall. Fellow AIAA.

measurements

$$\dot{x} = f(x, u) + w \tag{1}$$

$$z = h(x) + v \tag{2}$$

where $x \in \mathbb{R}^n$ is the state vector, $u \in \mathbb{R}^m$ is the control input vector, $z \in \mathbb{R}^r$ is the measurement vector, and $w \in \mathbb{R}^n$, $v \in \mathbb{R}^r$ are the process noise and the measurement noise vector, respectively. Both of them are random sequences with known probability distributions.

For stochastic optimization, the performance index to be minimized is defined as

$$J = E\left[\int_0^{t_f} L(x, u; t)\, \mathrm{d}t\right] \tag{3}$$

where L is a loss function, and the expectation is taken with respect to all underlying random variables. For convenience of mathematical description and numerical implementation, the discrete-time version of Eq. (3) is generally preferred. It has the form

$$J = E\left[L_N(x_N) + \sum_{k=0}^{N-1} L_k(x_k, u_k)\right] \tag{4}$$

The solution to this problem is of the form u_k^* for $k = 0, 1, \ldots, N-1$, where u_k^* is a control input sequence that minimizes Eq. (4). In principle, this problem can be solved as a dynamic programming problem. That is, let V_k be the minimum cost-to-go from k. Then the principle of optimality gives the backward recursive equation called the Bellman equation

$$V_k = \min_{u_k}\{E[L_k(x_k, u_k) + V_{k+1}|\mathcal{I}_k]\} \quad \text{for } k = N-1, N-2, \ldots, 0 \tag{5}$$

with the boundary condition given by

$$V_N = E[L_N(x_N, u_N)|\mathcal{I}_N] \tag{6}$$

Note that the expectation is conditioned on $\mathcal{I}_k$ in Eq. (5) which represents currently available information including the set of measurements and control inputs up to k. The optimal control u_k^* can be obtained by solving this dynamic programming problem formulated as Eqs. (5) and (6). However, numerical difficulties due to "the curse of dimensionality" make this problem practically unsolvable even for simple cases [4].

III. Previous Approaches

Since Feldbaum first discussed the concept of dual control in his seminal papers in 1960 and 1961 [1,2], a considerable amount of research has been performed on this topic. There are some simple problems for which optimal solutions have been obtained. A four-state Markov chain problem was solved by Sternby [6], and a first-order system with two possible gain values was treated by Bernhardsson [7]. Numerical solutions for some very simple adaptive dual-control problems have also been calculated [8]. However, they are exceptional cases, and problems of a reasonable size are practically unsolvable either analytically or numerically.

Various suboptimal techniques that possess some dual features have also been developed for adaptive and/or stochastic control applications. For more specific physical applications, missile interception using angle-only measurements has attracted some attention, and several dual-control guidance laws have been suggested [9,10]. Those techniques provide approximate solutions by adding perturbation signals, constraining the variance of the estimates, modifying the cost function, approximating a value function with a finite parameter set, etc.

There are two relatively common and intuitive approaches among them. The first is to add a probing input u_a to improve the observability of the system state. That is,

$$u_{\text{new}} = u_0 + u_a \tag{7}$$

where u_0 is the solution to a deterministic or cautious control problem, and u_a is an input that is designed separately based on a set of heuristics. The advantage of this approach is that it is simple. The disadvantage is that there is no systematic way of designing the u_a, and the overall performance depends heavily on the heuristics chosen.

The second method is to form a cost function that is the weighted sum of a standard cost J_0 (e.g., linear quadratic control) and a term that penalizes the system uncertainty J_a. That is,

$$J_{\text{new}} = J_0 + \lambda J_a \tag{8}$$

Often, a scalar function of the error covariance is used for J_a. The advantage of this approach is that it lends itself well to numerical search techniques. However, solutions are typically limited because the search space grows exponentially with respect to look-ahead time. Also, there is no systematic means of choosing the weighting parameter λ, and the resulting cost function might have little relevance to the true cost defined in Eq. (3).

Comprehensive overviews of various suboptimal techniques are available in [11,12].

IV. Suboptimal Stochastic Control

Proposed here is a suboptimal technique that offers an efficient and systematic method to generate an augmented cost function and to calculate probing inputs while minimizing a quadratic form of the cost defined in Eq. (3). The approach yields a feedback control solution of the form

$$u = -K_x\hat{x} - K_\lambda\lambda \tag{9}$$

where $\hat{x}$ is the estimated state calculated using a standard extended Kalman filter (EKF), and λ is a new state vector associated with the system uncertainties. The term $K_\lambda\lambda$ provides the inputs required to reduce the uncertainty, whereas the term $K_x\hat{x}$ drives the system to its desired state.

Details of this approach are presented in the following subsections. Section IV.A develops the performance index. Section IV.B defines an augmented state vector, which includes the system state and uncertainty state, and rewrites the performance index in terms of this new state vector. Sections IV.C and IV.D describe how the system state and the uncertainty state are propagated. Section IV.E summarizes the resulting control logic.

A. Performance Index

To define the quadratic cost function that will be used for optimization, consider the random variable x to be represented as a cloud of particles x_i, $i = 1, 2, \ldots, N$, which are distributed in state space as in Fig. 1.

Given this, the cost can be calculated as the sequential sum of squared distances between the desired state and each particle. The cost reflects both the distance between those particles and the desired state and how severely scattered they are. The quality of control at a

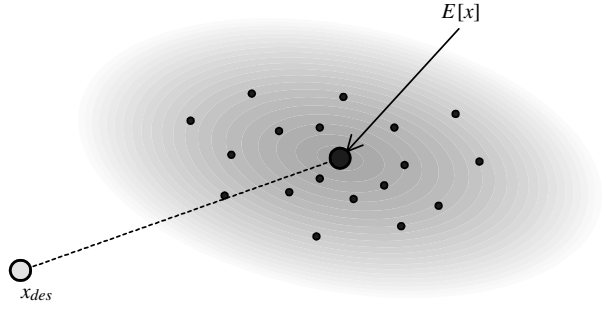

Fig. 1 Cloud of particles representing a distribution of the random variable x at a specific time.

particular time can be expressed using the following quadratic expression:

$$\delta J = \frac{1}{N}\sum_{i=1}^{N}\{(x_i - x_{\text{des}})^T Q_c (x_i - x_{\text{des}}) + u^T R_c u\}$$
$$= E[(x - x_{\text{des}})^T Q_c (x - x_{\text{des}}) + u^T R_c u] \tag{10}$$

where x_{des} is a desired state. Q_c and R_c are weighting matrices. The average operator $E[\cdot]$ works on samples only, not on time. Equation (10) can be rewritten as follows:

$$\delta J = (\hat{x} - x_{\text{des}})^T Q_c (\hat{x} - x_{\text{des}}) + u^T R_c u + E[(x - \hat{x})^T Q_c (x - \hat{x})]$$
$$= (\hat{x} - x_{\text{des}})^T Q_c (\hat{x} - x_{\text{des}}) + u^T R_c u + \text{tr}\{Q_c P_e\} \tag{11}$$

with $E[x] = \hat{x}$ and $P_e = E[\tilde{x}\tilde{x}^T] = E[(\hat{x} - x)(\hat{x} - x)^T]$.

The first two terms in Eq. (11) are in a familiar quadratic form. Expressing the third term in a quadratic form would enable solutions that exploit existing mathematical tools. This can be done by noting that the error covariance P_e is a positive semidefinite matrix, thus there exists a matrix S that satisfies $P_e = SS^T$. However, matrix square roots are not unique in general. For example, when S is a square-root matrix of P, then so is ST with T being an arbitrary orthonormal matrix. One option to secure the uniqueness of S is to express it as a lower triangular matrix for which the diagonal elements are positive. Also, by requiring (for convenience) that Q_c be a diagonal matrix, the last term in Eq. (11) is now expressed as

$$\text{tr}\{Q_c P_e\} = \text{tr}\{Q_c SS^T\} = \sum_{j=1}^{n}\left\{q_{jj}\left\{\sum_{k=1}^{j} s_{jk}^2\right\}\right\} \tag{12}$$

where $Q_e(i,i) = q_{ii}$ and $S(i,j) = s_{ij}$. Hence, Eq. (11) can now be rewritten as

$$\delta J = (\hat{x} - x_{\text{des}})^T Q_c (\hat{x} - x_{\text{des}}) + u^T R_c u + \sum_{j=1}^{n}\left\{q_{jj}\left\{\sum_{k=1}^{j} s_{jk}^2\right\}\right\} \tag{13}$$

This is the quadratic function of the estimated state deviation $(\hat{x} - x_{\text{des}})$, the control input u, and the new variable s associated with the square root of the error covariance matrix. Finally, integrating Eq. (13) along time yields the performance index to be minimized for stochastic optimization

$$J = \int_0^{t_f}\left\{(\hat{x} - x_{\text{des}})^T Q_c (\hat{x} - x_{\text{des}}) + u^T R_c u + \sum_{j=1}^{n}\left\{q_{jj}\sum_{k=1}^{j} s_{jk}^2\right\}\right\} \text{d}t \tag{14}$$

Note that, as a limiting case, when perfect estimation is achieved under no uncertainty ($\hat{x} \to x$, $s_{ij} \to 0$), Eq. (14) reduces to the quite familiar quadratic performance index for the deterministic system

$$J = \int_0^{t_f}\{(x - x_{\text{des}})^T Q_c (x - x_{\text{des}}) + u^T R_c u\}\,\text{d}t \tag{15}$$

The first two terms of Eq. (14) correspond to a certainty equivalence control cost, and the third term corresponds to the cost due to uncertainties in the system. By minimizing the summation of all these three terms, both the system's CE control cost and uncertainties can be reduced at the same time. A graphical interpretation of this cost is illustrated in Fig. 2. By minimizing the suggested stochastic control cost in Eq. (14), the probability distribution in Fig. 2a, which is wide and for which the center is off from the desired state value, becomes relatively sharper and closer to the desired state x_d, as shown in Fig. 2b.

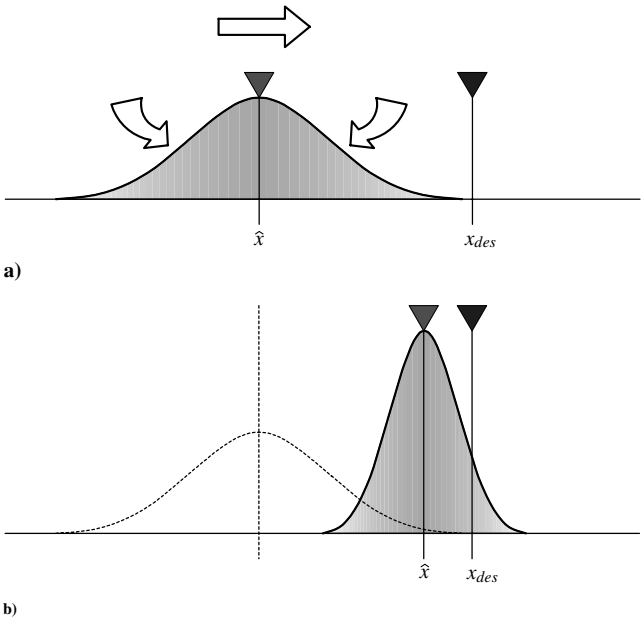

Fig. 2 Desired time propagation of a probability distribution function.

B. State Augmentation

The performance index in Eq. (14) can be expressed in a simpler form by representing the elements of S in a vector form. Specifically, given

$$S = \begin{bmatrix} s_{11} & 0 & 0 & \cdots & 0 \\ s_{21} & s_{22} & 0 & \cdots & 0 \\ s_{31} & s_{32} & s_{33} & \cdots & 0 \\ \vdots & \vdots & \vdots & \ddots & 0 \\ s_{n1} & s_{n2} & s_{n3} & \cdots & s_{nn} \end{bmatrix} \tag{16}$$

define λ as the single column vector that contains all the nonzero elements in S, and call this new vector an uncertainty state vector because it contains the information on the internal status of the system uncertainty. That is,

$$\lambda = [\, s_{11} \quad s_{21} \quad s_{22} \quad s_{31} \quad \cdots \quad s_{nn}\,]^T \tag{17}$$

where $\lambda \in \mathbb{R}^{n(n+1)/2}$.

The quadratic performance index in Eq. (14) then becomes (for descriptive convenience, the desired state x_{des} is set to zero hereafter without loss of generality)

$$J = \int_0^{t_f}\{\hat{x}^T Q_c \hat{x} + u^T R_c u + \lambda^T W_c \lambda\}\,\text{d}t \tag{18}$$

where

$$W_c = \begin{bmatrix} q_{11} & 0 & 0 & 0 & \cdots & 0 \\ 0 & q_{22} & 0 & 0 & \cdots & 0 \\ 0 & 0 & q_{22} & 0 & \cdots & 0 \\ 0 & 0 & 0 & q_{33} & \cdots & 0 \\ \vdots & \vdots & \vdots & \vdots & \ddots & 0 \\ 0 & 0 & 0 & 0 & \cdots & q_{nn} \end{bmatrix} \tag{19}$$

and $W_c \in \mathbb{R}^{[n(n+1)/2]\times[n(n+1)/2]}$. If Q_c is not a diagonal matrix, neither is W_c. However, it still can be represented as a quadratic expression shown in Eq. (18).

A more compact expression can be obtained through state augmentation. Denote the augmented state vector as

$$\xi = \begin{bmatrix} x \\ \lambda \end{bmatrix} \tag{20}$$

where $\xi \in \mathbb{R}^{n(n+3)/2}$, and the dimension $n(n+3)/2$ corresponds to the minimum number of states required to represent the stochastic system under the Gaussian distribution assumption. That is, the system has n state variables, and the error covariance matrix which is symmetric has $n(n+1)/2$ independent variables. With this, Eq. (18) can be rewritten as

$$J = \int_0^{t_f} \{\xi^T Q_a \xi + u^T R_c u\}_{x=\hat{x}} \, \mathrm{d}t \tag{21}$$

where

$$Q_a = \begin{bmatrix} Q_c & 0 \\ 0 & W_c \end{bmatrix}$$

C. Extended Kalman Filter

The control law defined in Eq. (9) requires the propagation of states $\hat{x}$ and λ. To calculate $\hat{x}$, the EKF is used here because nonlinearities are assumed to be present in the state or/and measurement equation. The random sequences w in Eq. (1) and v in Eq. (2) are assumed to have zero mean Gaussian distributions given by $w \sim \mathcal{N}(0, Q_e)$ and $v \sim \mathcal{N}(0, R_e)$.

The differential equations for updating state estimate $\hat{x}$ and error covariance matrix P_e are

$$\dot{\hat{x}} = f(\hat{x}, u) + P_e H^T R_e^{-1}[z - h(\hat{x})] \tag{22}$$

$$\dot{P}_e = FP_e + P_e F^T + Q_e - P_e H^T R_e^{-1} H P_e \tag{23}$$

where

$$F = \left.\frac{\partial f(x,u)}{\partial x}\right|_{x=\hat{x}} \qquad H = \left.\frac{\partial h(x)}{\partial x}\right|_{x=\hat{x}}$$

Because uncertainties are associated with the square root of the error covariance matrix, the use of the square-root Kalman filter algorithm for the state estimation is appropriate. It is algebraically equivalent to the standard Kalman filter. Details are given in the next section.

Note that, instead of the EKF, an alternative filtering algorithm such as the unscented Kalman filter (UKF) can also be used here. Whereas the EKF is based on approximating the nonlinearities by the first-order Taylor series expansion, the UKF is known to be capable of capturing the posterior mean and covariance accurately to the third order [13]. Some performance improvement might be gained by exploiting such an advanced filtering technique. The replacement can be done by substituting the corresponding UKF formulations for the EKF formulations described in Secs. IV.C and IV.D. See [14] for the square-root algorithm of the UKF.

D. Propagation of the Uncertainty States

To propagate λ, note that the first-order time derivative of the augmented state vector is

$$\dot{\xi} = \begin{bmatrix} \dot{x} \\ \dot{\lambda} \end{bmatrix} \triangleq \begin{bmatrix} f \\ g \end{bmatrix} = \eta(\xi, u) \tag{24}$$

where g is an enumeration of the first-order time derivatives of the square-root error covariance matrix

$$g = [\, \dot{s}_{11} \quad \dot{s}_{21} \quad \dot{s}_{22} \quad \dot{s}_{31} \quad \cdots \quad \dot{s}_{nn} \,]^T$$

and

$$\dot{s}_{ij} = \dot{S}(i,j)$$

With the definition $P = SS^T$, the differential Riccati equation becomes

$$\dot{P} = \dot{S}S^T + S\dot{S}^T = (F - \tfrac{1}{2}SS^T H^T R^{-1} H)SS^T + \tfrac{1}{2}QS^{-T}S^T + SS^T(F^T - \tfrac{1}{2}H^T R^{-1} H S S^T) + \tfrac{1}{2}S^{-T}S^T Q \tag{25}$$

and the matrix differential equation that is satisfied by the particular solution is given by

$$\dot{S} = (F - \tfrac{1}{2}SS^T H^T R^{-1} H)S + \tfrac{1}{2}QS^{-T} \tag{26}$$

However, careful treatment is required when propagating S along time, because $\dot{S}$ may not be lower triangular even though S is.

An efficient method for computing $\dot{S}$ in a lower triangular form has been suggested by Morf et al. [15], which guarantees the uniqueness of S. $\dot{S}$ in a lower triangular can be expressed in the following form:

$$\dot{S} = S[M]^{+/2} \tag{27}$$

where

$$M \triangleq S^{-1}(\dot{S}S^T + S\dot{S}^T)S^{-T} = S^{-1}\dot{S} + \dot{S}^T S^{-T} = S^{-1}FS + S^T F^T S^{-T} - S^T H^T R^{-1} H S + S^{-1} Q S^{-T} \tag{28}$$

and the operator $[\cdot]^{+/2}$ is defined by

$$[U]_{ij}^{+/2} = \begin{cases} \frac{1}{2}u_{ij} & \text{for } i = j \\ u_{ij} & \text{for } i < j \\ 0 & \text{otherwise} \end{cases}$$

for an arbitrary matrix U.

Because the uncertainty states are obtained from the square root of the error covariance matrix, it is more effective and convenient to use the square-root filter formulation than the standard Kalman filter formulation. This substitution brings a couple of advantages. First, the increase in computational load is minimal, because few redundant filter-related calculations are required. Second, the square-root filter is known to have better properties in accuracy and stability than the standard Kalman filter [16].

E. Suboptimal Controller

Finally, the optimization problem can be summarized as follows:

Find the optimal control input history $u^*(t)$ for $0 \le t < t_f$ that satisfies

$$u^* = \arg\min_u \int_0^{t_f} \{\xi^T Q_a \xi + u^T R_c u\} \, \mathrm{d}t \tag{29}$$

subject to

$$\dot{\xi} = \eta(\xi, u) \tag{30}$$

Because of the approximation involved in the covariance propagation step and the complexity of its state-space representation, it can be a difficult task to calculate the optimal solution to this nonlinear control problem. However, several techniques are available to obtain suboptimal solutions.

In this study, state-feedback control using an infinite horizon steady-state gain is used. This gain is computed as follows. Assume that the differential Riccati equation for the preceding optimization problem has a limiting solution P_c which satisfies the algebraic Riccati equation (ARE)

$$0 = A^T P_c + P_c A + Q_a - P_c B R_c^{-1} B^T P_c \tag{31}$$

where

$$A = \left.\frac{\partial \eta(\xi,u)}{\partial \xi}\right|_{x=\hat{x}} \qquad B = \left.\frac{\partial \eta(\xi,u)}{\partial u}\right|_{x=\hat{x}}$$

Then K is simply the steady-state Kalman gain matrix:

$$K = R_c^{-1} B^T P_c \tag{32}$$

The gain matrix K is calculated at every time step.

The final result is the time-varying, suboptimal, state-feedback control law

$$u = -K(\xi - \xi_{ss})|_{x=\hat{x}} = -K_x(\hat{x} - x_{\text{des}}) - K_\lambda(\lambda - \lambda_{ss}) \tag{33}$$

where

$$K = [\, K_x \quad K_\lambda \,]$$

and λ_{ss} is obtained from the steady-state solution of Eq. (23).

The resulting LQD control block diagram is shown in Fig. 3. It includes two distinctive feedback terms, K_x and K_λ. K_x focuses primarily on the control goal of stabilization, and K_λ provides an additional feedback input driven by the uncertainty state, which decreases uncertainties of the control system in a direct manner and improves the control performance indirectly.

V. Monocular Vision-Based Docking Application

The developed dual-control algorithm LQD is applied here to a monocular vision-based docking problem. The problem is formulated and its state-space representation is presented. Also, a docking scenario for the simulations and experiments for the following sections is illustrated. Finally, a series of numerical simulations and experimental test results are presented.

A. Problem Formulation

For the vehicle, a four-wheeled rover is considered (Fig. 4). The vehicle is assumed to be rear-wheel steering to be consistent with typical dynamic vehicles (e.g., rudder-steered vehicles such as ships and airplanes) considered for future experimental implementation.

The equations of motion in polar coordinates are

$$\dot{\mathbf{x}} = \begin{bmatrix} \dot{\rho} \\ \dot{\beta} \\ \dot{\psi} \\ \dot{V} \end{bmatrix} = \begin{bmatrix} -V\cos(\beta - \psi) \\ (V/\rho)\sin(\beta - \psi) \\ -(V/l_a)\tan\delta \\ -(1/T_v)(V - V_c) \end{bmatrix} \tag{34}$$

where ρ, β, and ψ are the range, bearing, and heading, respectively, l_a is the distance between the front and rear axles, and δ is the steering angle. The speed change dynamics is approximated as a first-order system. V and V_c are the actual speed and the speed command input, respectively, and T_v is the time constant. The control input vector constituted by δ and V_c can be represented as

$$u = [\, \delta \quad V_c \,]^T \tag{35}$$

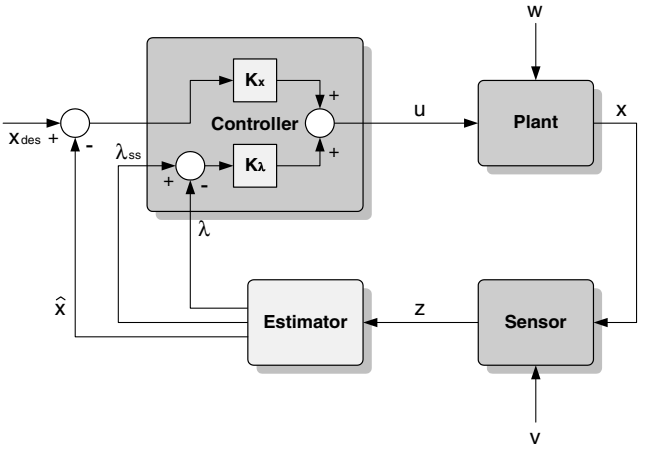

Fig. 3 Control block diagram with the LQD controller.

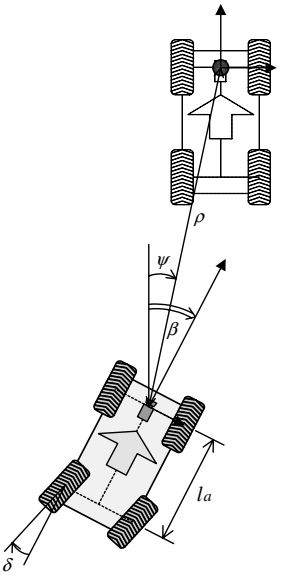

Fig. 4 Four-wheeled rover configuration.

For sensing, monocular vision, heading angle, and speed measurements are assumed to be available. The measurement equation is given by

$$\mathbf{z} = \begin{bmatrix} z_1 \\ z_2 \\ z_3 \end{bmatrix} = \begin{bmatrix} \beta - \psi \\ \psi \\ V \end{bmatrix} \tag{36}$$

Note that the vision measurement z_1 is expressed as $(\beta - \psi)$, where $\beta = \tan^{-1}(y/x)$, which is the angle difference between bearing and heading. The vision sensor (e.g., camera) is assumed to be fixed to the vehicle, consequently, the angle difference between bearing and heading is an actual measurement from the sensor.

The design procedure of the LQD controller for this system begins with system state augmentation. Given the system equations of the monocular vision-based docking problem, the augmented state

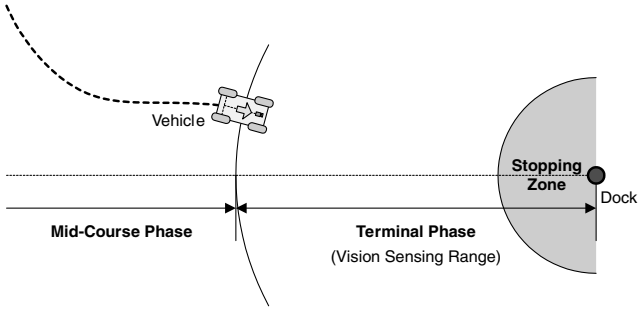

Fig. 5 Docking scenario.

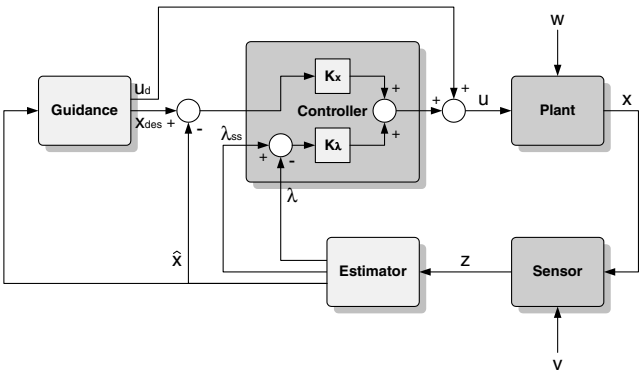

Fig. 6 Control block diagram of the docking controller.

Table 1 Simulation parameter settings

Parameter	Symbol	Value
Wheelbase	l_a, m	0.335
Max. steering angle	$\delta_{\max}$, deg	16.0
Half-view angle	$\sigma_{\max}$, deg	30.0
Design speed	V_s, m/s	0.3
Time constant	T_v, s	0.2
State weighting	Q_c	Diag{9.0, 1.0, 1.0, 1.0}
Control weighting	R_c	Diag{100.0, 100.0}
Error covariance (disturbance)	Q_e	Diag{10^{-5}, 10^{-5}, 10^{-5}, 10^{-5}}
Error covariance (measurement noise)	R_e	Diag{0.0012, 3.0462, 0.0001}
Error covariance (initial state)	P_0	Diag{2.25, 0.0076, 0.0003, 0.01}

vector is defined as

$$\xi = [\,x \quad | \quad \lambda\,]^T \in \mathbb{R}^{14}$$
$$= [\,\rho \quad \beta \quad \psi \quad V \quad s_{11} \quad s_{21} \quad s_{22} \quad s_{31} \quad \cdots \quad s_{44}\,]^T \qquad (37)$$

where

$$S = \begin{bmatrix} s_{11} & 0 & 0 & 0 \\ s_{21} & s_{22} & 0 & 0 \\ s_{31} & s_{32} & s_{33} & 0 \\ s_{41} & s_{42} & s_{43} & s_{44} \end{bmatrix}$$

and

$$\lambda = [\,s_{11} \quad s_{21} \quad s_{22} \quad s_{31} \quad \cdots \quad s_{44}\,]^T$$

The original system has a dimension of four, and the uncertainty state has a dimension of $n(n+3)/2 = 10$. The resulting augmented system has a dimension of $n(n+3)/2 = 14$.

Once the augmented system is obtained, the systematic control input calculation, along with the associated state estimation, can be performed following the procedure shown previously.

B. Docking Scenario

Assume that the vehicle has been driven to a point from which the target is visible by the vehicle's onboard camera (see Fig. 5). This is the point where the LQD controller takes over the control authority.

At the start of this terminal phase, the vehicle is located at a certain distance away from the target dock. The distance to the dock is initially unknown, but the presence of the dock is identifiable from the camera, and so the relative bearing angle to the docking target, with some measurement error due to the finite resolution of the camera, is available. Also available is a rough approximation of range based on the size of the dock in the camera image. Thus, the estimator can be appropriately initialized to prevent premature filter divergence.

During the terminal phase, the dual controller generates control inputs for the vehicle. Once the vehicle passes the boundary of the stopping zone, the vehicle is ordered to reduce its speed and start decelerating. Finally, the vehicle is commanded to stop just before collision occurs, and success of a docking trial is evaluated based on the errors in final vehicle position and orientation relative to the desired values depending on the dock type.

The size of the stopping zone is determined considering the vehicle's stopping capability and the stability properties of the filter system. As shown in Eq. (34), the system is highly nonlinear. The nonlinearity becomes even more significant as the vehicle approaches the dock at the origin. To avoid filter instability, the filter is turned off and the dead reckoning approach is taken in the stopping zone.

Also, to improve the overall docking performance, especially at the final stage of docking where the level of uncertainty is very low, a feedforward control scheme based on the proportional navigation guidance law, which is widely used for the terminal guidance of missiles, is added to the proposed LQD control system as shown in Fig. 6. However, the addition is a practical refinement, not a required component of the overall control system.

VI. Simulation

For the simulation, nonzero error covariance matrices are considered, and artificial system disturbance and measurement noise are injected to the simulation model using random numbers. Results are generated for three different methods to provide a basis for comparison. The simulation parameter settings are shown in Table 1.

A. Simulation Results

It is assumed that the vehicle is initially aligned to the centerline of the target dock. In this setting, conventional CE controllers generate a straight-line path of approach toward the dock, and do not allow the state estimator to extract range information using a vision sensor.

Simulation results using a conventional CE controller, specifically an LQG, are presented in Fig. 7. As expected, the system uncertainty

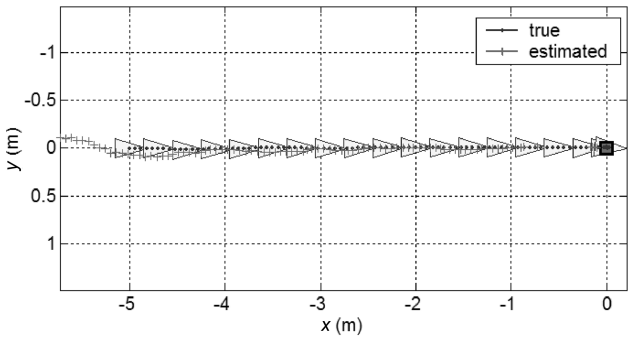

a) Docking trajectory

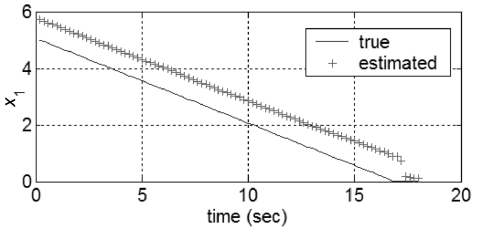

b) ρ: range (m)

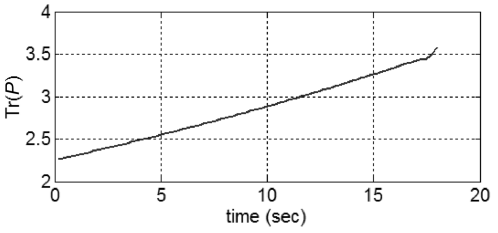

c) Tr (P): uncertainty level

Fig. 7 CE control ($\rho_0 = 5$, $\beta_0 = 0$, $\psi_0 = 0$, $\psi_{\text{final}} = 0$).

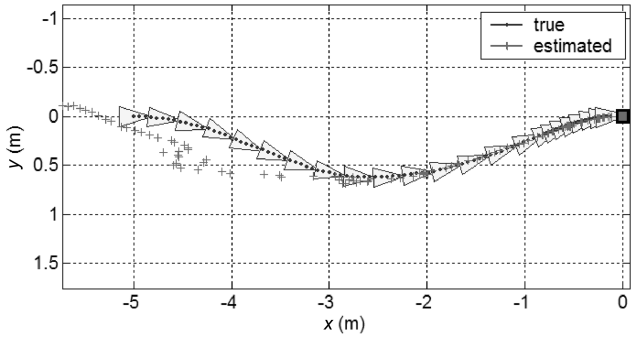

a) Docking trajectory

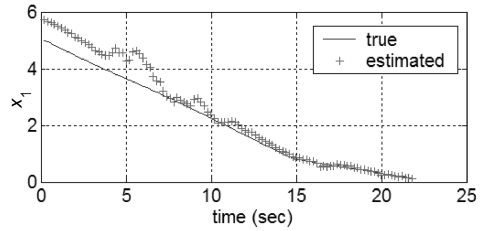

b) ρ: range (m)

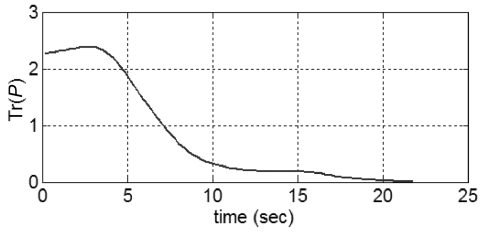

c) Tr (P): uncertainty level

Fig. 8 LQD control ($\rho_0 = 5$, $\beta_0 = 0$, $\psi_0 = 0$, $\psi_{\text{final}} = 0$).

continually increases, as shown in Fig. 7c, due to the lack of range observability and nonzero process noise, and little improvement is observed for the range estimate for most of the trajectory (see Fig. 7b). For this specific case, the estimate converges at the last moment when the vehicle gets very close to the target dock. However, the sudden converge of the range estimate does not allow sufficient time nor space to take action preventing collision. This can cause serious operational difficulties for docking of an actual vehicle, often with a large inertia and limited maneuverability.

Simulation results of the new LQD controller are shown in Fig. 8. The nonzero initial error covariance drives the vehicle to swerve off of the dock centerline and take a probing motion. As the magnitude of the vehicle's lateral motion increases, the system uncertainty measure Tr(P) in Fig. 8c rapidly decreases, and the estimated range converges to the true state value as shown in Fig. 8b. Once sufficient information on the relative position is obtained, the vehicle moves back to the centerline to meet the final heading condition and, at the same time, its speed is reduced.

B. Performance Analysis

A quantitative performance comparison is made between the LQD approach and the two different search-based approaches: a look-ahead search and an exhaustive breadth-first search.

Table 2 Performance index and run-time cost

Controller	Cost J	Run time
LQD	3837.9	1.00
Look-ahead search ($p = 1$)	5205.2	0.77
Look-ahead search ($p = 5$)	4851.0	1.78
Look-ahead search ($p = 20$)	3958.5	9.41
Exhaustive search ($t_{\text{sec}} = 0.5$, $n_{\text{sec}} = 4$)	3822.8	394.58
Exhaustive search ($t_{\text{sec}} = 0.7$, $n_{\text{sec}} = 5$)	3797.1	4136.39

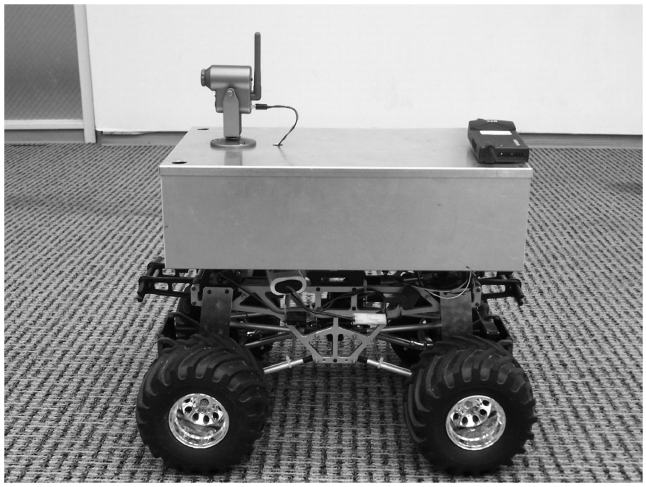

Fig. 9 Aerospace Robotics Laboratory rover: four-wheel drive vehicle, with a rear-wheel steering configuration adopted like a forklift. Camera is installed on the front-axle line.

The first controller for comparison adopts a look-ahead search:

$$u^* = \arg \min_{u_m,\ldots,u_{m+p-1}} \left\{ E\left[\sum_{k=m}^{m+p} L_k(x_k, u_k) \middle| \mathcal{I}_m \right] \right\} \tag{38}$$

where p is the look-ahead parameter. The simplest form of this search is obtained by setting $p = 1$, called the one-step-look-ahead search. As p increases, the search problem soon becomes intractable. In this study, for each finite look-ahead time interval, constant control inputs are assumed to be maintained. For a specific optimization technique, the gradient descent method with a variable step-size is used.

The second controller for comparison is an exhaustive search:

$$u^* = \arg \min_{u_0,\ldots,u_{N-1}} \left\{ E\left[L_N(x_N) + \sum_{k=0}^{N-1} L_k(x_k, u_k) \middle| \mathcal{I}_N \right] \right\} \tag{39}$$

The exhaustive search requires huge computational effort, and thus cannot be used as a real-time controller. However, a control trajectory closer to the optimum is expected to be found through this approach. To keep computation time manageable, the search is performed for the first few seconds during which the choice of control input is relatively critical. For the remaining time, proportional navigation guidance, which is widely used as a terminal controller, is applied.

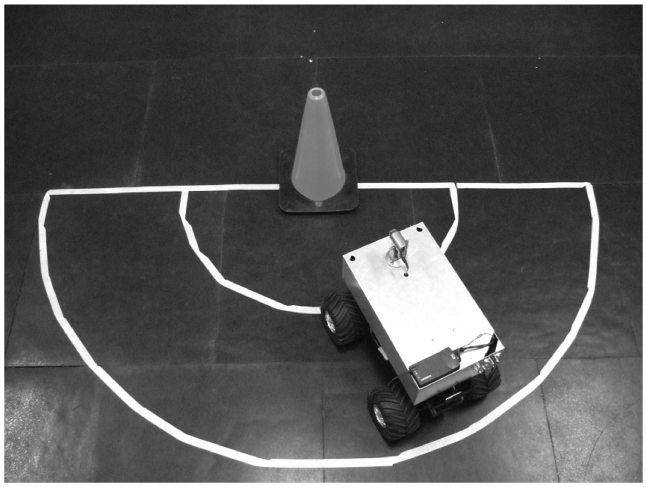

Fig. 10 Docking target: Two concentric semicircles ($R_{\text{inner}} = 0.5$ m and $R_{\text{outer}} = 1.0$ m) are drawn around the pylon to exhibit final docking performance more clearly.

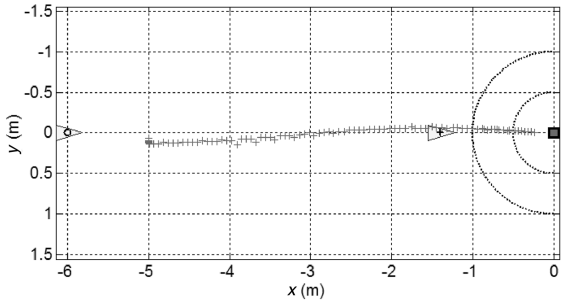

a) Docking trajectory

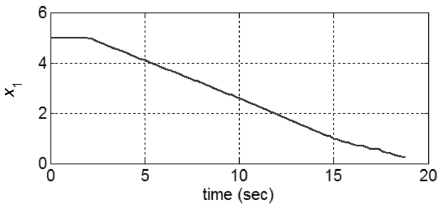

b) ρ: range

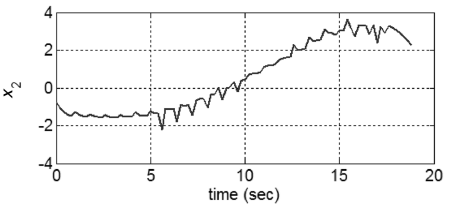

c) β: bearing angle (deg)

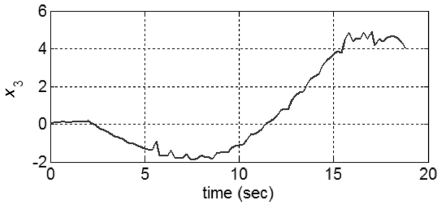

d) ψ: heading angle (deg)

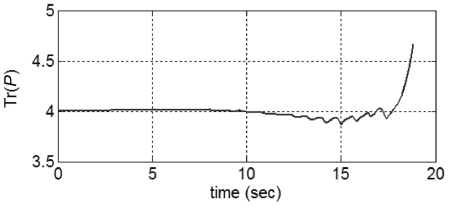

e) Tr(P): uncertainty

Fig. 11 CE control for directional docking (initial position: $x_{0,\text{filter}} = -5$ m, $x_{0,\text{actual}} = -6$ m).

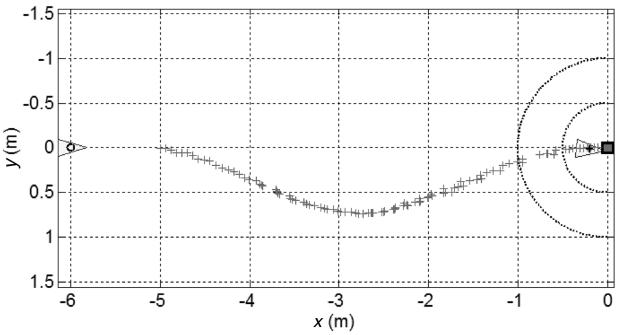

a) Docking trajectory

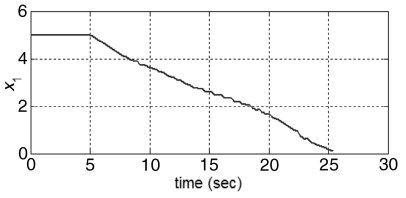

b) ρ: Range

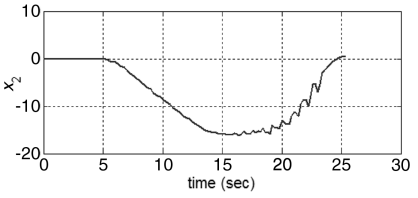

c) β: Bearing angle (deg)

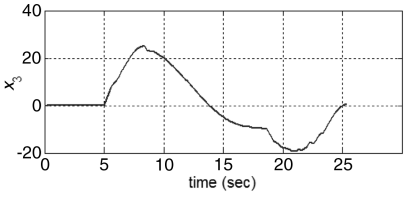

d) ψ: Heading angle (deg)

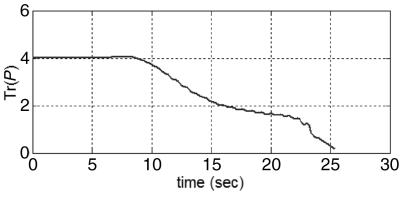

e) Tr (P): Uncertainty

Fig. 12 LQD control for directional docking (initial position: $x_{0,\text{filter}} = -5$ m, $x_{0,\text{actual}} = -6$ m).

Table 2 presents the results of the comparisons. Here, p represents the look-ahead step parameter. The parameters for the exhaustive search are t_{sec} and n_{sec}: the duration of each time section and the number of time sections, respectively. The performance of the LQD controller compares favorably with the search-based methods when considering the run time and the accumulated cost.

VII. Experimental Test

The performance and validity of the developed dual-control algorithm are experimentally demonstrated and checked through a physical implementation of the vision-based docking system using a wheeled robot.

A. Experimental System

For the vehicle for docking, a four-wheeled rover equipped with motions sensors such as a wheel encoder and a magnetic compass is used. Also, a wireless webcam is installed on the rover as a monocular vision sensor (see Fig. 9).

The target dock is represented by a pylon as shown in Fig. 10. The color segmentation method is applied to detect the target from the captured vision image.

B. Test Results

Again, runs with the CE controller were performed together with the LQD controller for comparison. The tests were performed varying the vehicle's initial position in the longitudinal direction. The result shown here is for the case with 1 m initial range estimate error. That is, the assumed initial range is 5 m, but the actual initial distance to the target is 6 m.

First, the test run results for the CE controller, specifically LQG, are shown in Fig. 11. No probing motion was taken, and the vehicle basically performed dead reckoning navigation with a large uncertainty remaining in the range direction. As can be seen from the figure, the uncertainty level does not decrease during the vehicle's approach, and the vehicle stops well ahead of the goal state. The initial range error remains approximately the same throughout the run.

The range state is unobservable and indistinguishable on the straight-line approach path generated by this type of controller. The range state is estimated based on the combination of the initial estimate and the integration of speed measurement information, for which the error is susceptible to noise and disturbance. As a result, satisfactory docking performance can never be guaranteed, even with a correct initial range estimate.

The experiment for the same initial condition was performed using the LQD controller. The results are shown in Fig. 12. Nonzero initial uncertainty drives the LQD controller to generate nonzero control inputs, thus the vehicle swerves off from the dock centerline and performs exploratory motion. This leads to the decrease of uncertainty level, as shown in Fig. 12e. Unlike the CE case in Fig. 11, even with this error in the initial range estimate, the vehicle successfully reaches the dock.

VIII. Conclusions

In this study, a new stochastic control algorithm for dual-control problems called LQD has been developed and presented. The controller design procedure of the new algorithm is different from existing suboptimal approaches and avoids the drawbacks of those techniques. The controller design procedure for the LQD algorithm is quite generic and systematic, and the resulting controller has a simple and intuitive form. It is expressed as the linear sum of a conventional CE control and an additional control term which responds to the level of uncertainty in the system.

Thus, the LQD controller can be applied to a wide class of control problems which exhibit the dual effect. In this paper, the algorithm was applied to the monocular vision-based docking application, which represents an extreme case of docking under limited sensing capability. Numerical stochastic simulations were carried out to evaluate the performance and validity of the new dual-control algorithm. Also, a series of experimental tests using a vision sensor and a mobile rover equipped with an odometer and a compass were performed. The test results demonstrated that the overall docking control system based on the LQD algorithm has sufficient real-time capability and robustness to measurement noise and uncertainties.

Although the proposed LQD algorithm is capable of overcoming the drawbacks and limitations of existing dual-control approaches, the limitations of the underlying approximate solution techniques such as the EKF and the ARE techniques may impose restrictions on the overall performance of the proposed LQD algorithm. Different underlying solution techniques that are more effective and efficient in dealing with nonlinear systems can be used to achieve improved stochastic control performance, to which future research can be directed.

References

[1] Feldbaum, A. A., "Dual Control Theory I–II," *Automation and Remote Control*, Vol. 21, 1960, pp. 874–880, 1033–1039.

[2] Feldbaum, A. A., "Dual Control Theory III–IV," *Automation and Remote Control*, Vol. 22, 1961, pp. 1–12, 109–121.

[3] Tse, E., Bar-Shalom, Y., and Meier, L., III, "Wide-Sense Adaptive Dual Control for Nonlinear Stochastic Systems," *IEEE Transactions on Automatic Control*, Vol. 18, No. 2, April 1973, pp. 98–108. doi:10.1109/TAC.1973.1100238

[4] Kirk, D. E., *Optimal Control Theory*, Prentice–Hall, Englewood Cliffs, NJ, 1970.

[5] Bryson, A. E., and Ho, Y. C., *Applied Optimal Control*, Hemisphere, New York, 1975, pp. 131–141.

[6] Sternby, J., "A Simple Dual Control Problem with an Analytical Solution," *IEEE Transactions on Automatic Control*, Vol. 21, No. 6, Dec. 1976, pp. 840–844. doi:10.1109/TAC.1976.1101383

[7] Bernhardsson, B., "Dual Control of a First-Order System with Two Possible Gains," *International Journal of Adaptive Control and Signal Processing*, Vol. 3, No. 1, 1989, pp. 15–22. doi:10.1002/acs.4480030103

[8] Åström, K. J., and Wittenmark, B., *Adaptive Control*, 2nd ed., Addison Wesley, Reading, MA, 1995, pp. 365–370.

[9] Casler, R. J., Jr., "Dual-Control Guidance Strategy for Homing Interceptors Taking Angle-Only Measurements," *Journal of Guidance, Control, and Dynamics*, Vol. 1, No. 1, 1978, pp. 63–70. doi:10.2514/3.55744

[10] Hull, D. G., Speyer, J. L., and Burris, D. B., "Linear-Quadratic Guidance Law for Dual Control of Homing Missiles," *Journal of Guidance, Control, and Dynamics*, Vol. 13, No. 1, 1990, pp. 137–144. doi:10.2514/3.20527

[11] Wittenmark, B., "Adaptive Dual Control Methods: An Overview," *Proceedings of the 5th IFAC Symposium on Adaptive Systems in Control and Signal Processing*, 1995, pp. 62–72, http://citeseerx.ist.psu.edu/viewdoc/summary?doi=10.1.1.25.7446.

[12] Unbehauen, H., "Adaptive Dual Control Systems: A Survey," *Proceedings of Adaptive Systems for Signal Processing, Communications, and Control Symposium 2000*, 2000, pp. 171–180. doi:10.1109/ASSPCC.2000.882466

[13] Julier, S. J., and Uhlmann, J. K., "Unscented Filtering and Nonlinear Estimation," *Proceedings of the IEEE*, Vol. 92, No. 3, 2004, pp. 401–422. doi:10.1109/JPROC.2003.823141

[14] Merwe, R., and Wan, E. A., "The Square-Root Unscented Kalman Filter for State and Parameter Estimation," *Proceedings of the IEEE International Conference on Acoustics, Speech, and Signal Processing*, 2001, pp. 3461–3464, http://citeseerx.ist.psu.edu/viewdoc/summary?doi=10.1.1.3.2168.

[15] Morf, M., Levy, B., and Kailath, T., "Square-Root Algorithms for the Continuous-Time Linear Least-Square Estimation Problem," *IEEE Transactions on Automatic Control*, Vol. 23, No. 5, Oct. 1978, pp. 907–911. doi:10.1109/TAC.1978.1101862

[16] Maybeck, P. S., *Stochastic Models, Estimation, and Control*, Vol. 1, Academic Press, New York, 1979, pp. 368–409.